

Modeling of Exciton Diffusion in Amorphous Organic Thin Films

Conor Madigan and Vladimir Bulović*

*Lab of Organic Optics and Electronics, Department of Electrical Engineering and Computer Science,
Massachusetts Institute of Technology, Cambridge, Massachusetts 02139, USA*

(Received 30 June 2005; published 31 January 2006; corrected 1 February 2006)

Time-resolved photoluminescence spectroscopy of amorphous organic thin films of aluminum tris-(8-hydroxyquinoline) show emission spectra that redshift with time following excitation by ultrafast laser pulses. Based on reports of similar phenomena in other materials, we attribute this effect to the exciton diffusion between energetically dissimilar molecules by means of Förster transfer. In analyzing results at 295, 180, 75, and 35 K, we show that existing theoretical treatments of exciton diffusion require two modifications to self-consistently fit our data: one must include spatial disorder in the model, and the energy dependence of Förster transfer must be calculated using the donor-acceptor spectral overlap, instead of a Boltzmann distribution. Monte Carlo simulations utilizing these changes yield results that are self-consistent with the observed spectral shifts.

DOI: 10.1103/PhysRevLett.96.046404

PACS numbers: 71.35.Aa, 33.20.Kf, 78.66.Qn

Optical and electrical response of organic optoelectronic devices is often controlled by the diffusion of excitons in the constituent materials. For example, in light emitting diodes, exciton diffusion affects the degree of cascade energy transfer and the color saturation, and in solar cells and photodetectors, exciton diffusion to interfaces is the central process in determining the exciton dissociation efficiency, and the consequent photogeneration efficiency. In addition, the improper modeling of exciton diffusion can lead to errors in the interpretation of experiments probing material physics, as in, for instance, the time and temperature dependence of luminescence and calculation of Förster radii. In this work we extend and correct the earlier theoretical models of exciton diffusion in amorphous organic thin film structures by utilizing a Monte Carlo (MC) simulation of the process and testing it against temperature dependent exciton diffusion data.

Exciton diffusion has been studied in disordered organic solids for decades, initially with work on organic crystals. Recently focus has shifted to amorphous organic materials where each molecule is subject to energetic and spatial disorder. One of the key advances in modeling exciton diffusion is the study of Movaghar *et al.*, which reports both MC simulation and a numerical analytic theory describing diffusion and energy relaxation of singlet excitons by Förster energy transfer [1–5]. The exciton transfer rate W between two molecules is given by

$$W = \chi(R)P(\epsilon_d, \epsilon_a), \quad (1)$$

where

$$P(\epsilon_i, \epsilon_j) = \begin{cases} \exp[-(\epsilon_a - \epsilon_d)/k_B T] & \epsilon_a > \epsilon_d \\ 1 & \text{otherwise} \end{cases}, \quad (2)$$

$$\chi(R) = (1/\tau)(R_F/R)^6, \quad (3)$$

τ is the radiative lifetime, k_B is Boltzmann's constant, R is the separation distance between the two molecules, T is the

temperature, ϵ_d and ϵ_a are the energies of the exciton donating and exciton accepting molecules, respectively, and R_F is the Förster radius. The excitonic density of states (DOS), $g(E)$, reflecting the energetic disorder of the system, was assumed to be Gaussian, with w_{DOS} denoting the full width half maximum (FWHM) of the distribution. It is further assumed that every molecule in the system has absorption and emission spectra of the same *shape* but different mean energy, such that the distribution of mean energies comprises $g(E)$.

Movaghar *et al.* predicted that, given a manifold of exciton energies described by $g(E)$, excitons relax towards a thermodynamic equilibrium energy over time. It was also reported that the mean exciton energy evolves towards lower energies roughly following $\exp[-ct]$ behavior, where c is a constant. Finally, the model predicts that the energy relaxation should increase as the temperature is reduced. Many subsequent studies of time-resolved photoluminescence (PL) spectroscopy reported dynamic spectral redshifts and qualitatively explained the data with models like the one reported by Movaghar *et al.* [6–14]. However, the power of the Movaghar *et al.* work arguably lies in the potential to quantitatively analyze energy shifts as a function of time, which, if experimentally verified, would provide a direct view of exciton diffusion in amorphous organic materials. To date, however, such direct quantitative fits have not been carried out.

In this study we perform a quantitative test of the Movaghar *et al.* model by comparing its predictions to the measured time dependent energy shifts in PL of fluorescent thin films of aluminum tris-(8-hydroxyquinoline) (AlQ3) at different temperatures. We find that self-consistent fits to the data are possible only if the theory is modified in two key respects. First, the analytic model presented by Movaghar *et al.* is consistent with MC simulations only for an ordered cubic lattice of molecular sites, and we find that a spatially random lattice of sites is

required to accurately model exciton diffusion by Förster transfer in amorphous AlQ3 thin films, as discussed below [15]. Second, in the Movaghar *et al.* model the energy dependence of the exciton transfer rate is approximated by a Boltzman distribution [as expressed in Eq. (2)]. This differs from the exact energy dependence for Förster transfer given by

$$R_F^6 = \frac{9}{8\pi} \frac{c^4}{n^4} \kappa^2 \int \frac{S_D(\omega)\sigma_A(\omega)}{\omega^4} d\omega, \quad (4)$$

where c is the speed of light, n is the bulk film refractive index, κ is a orientation factor, S_D is the normalized molecular donor emission spectrum, and σ_A is the molecular acceptor absorption cross section [18]. Assuming that the excitonic energy disorder leads to similar shifts in the mean energies of absorption and emission spectra of individual molecules, then Eq. (4), indeed, yields a transfer rate that favors downhill energy transfer. Very rarely, however, would the functional form of that energy dependence be the same as for a Boltzman distribution. We find below that the use of a Boltzman distribution is, indeed, an inadequate approximation to the energy dependence of exciton diffusion in AlQ3.

We measure time-resolved PL of 100 nm films of AlQ3 grown by vacuum thermal evaporation ($\leq 1 \times 10^{-6}$ Torr growth pressure and growth rates of ≈ 0.2 nm/s) on clean glass substrates. Following film growth, the samples were briefly exposed to atmosphere during transfer from the growth chamber into a closed cycle helium cryostat. AlQ3 thin film PL is excited with 100 fs long, 395 nm wavelength laser pulses generated by frequency doubling the output of a Coherent RegA 9000 regenerative amplifier seeded by a Coherent Mira 900F mode locked Ti:sapphire laser. A repetition rate of 250 kHz was used for all measurements. The fluorescence was detected using a Hamamatsu C4780 picosecond fluorescence lifetime system consisting of a C4334 streak camera and a C5094 spectrograph. The time resolution was limited by triggering jitter to 100 ps. The spectrograph grating set the wavelength resolution to 0.2 nm. All of the measurements were integrated over 50 000 frames at a frame capture rate of 30 Hz. The samples were kept under vacuum in the cryostat at all times, and no sample degradation was observed during any of the measurements.

Time-resolved measurements were taken at temperatures of 295, 180, 75, and 35 K. Time integrated spectra for each temperature are shown in Fig. 1. For each measurement, the time-resolved PL shifts to lower energies with increasing time, as shown by the plots of the mean PL energy as a function of time in Fig. 2. Note that the data are plotted on a logarithmic time scale, indicating that the rate of spectral shifting decreases with time. In addition, absorption spectra were taken at each temperature using a Cary 5000 (also shown in Fig. 1).

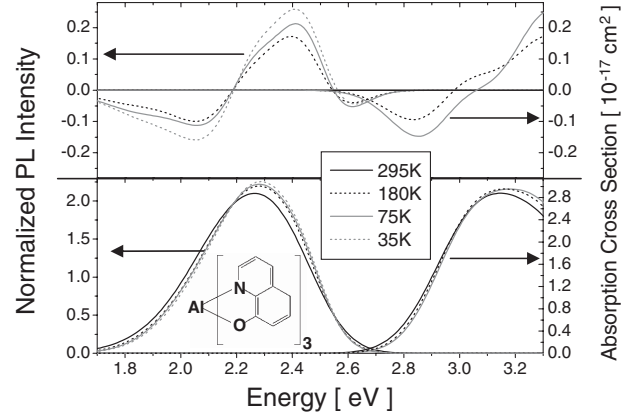


FIG. 1. PL and absorption spectra for 100 nm films of AlQ3 at temperatures of 295, 180, 75, and 35 K, where the PL spectra are time integrated over the entire emission pulse and normalized to integrate over energy to unity. The bottom panel shows the spectra themselves, while the top panel shows the deviation of the cooled spectra from the 295 K spectra, to better illustrate the differences between the temperatures. To within the measurement error, the absorption spectra at 35 and 75 K are identical. Inset: chemical structure of AlQ3.

We compare the experimental data to the Movaghar *et al.* model, hereafter referred to as model I, and also to our MC simulation utilizing a disordered lattice of sites and a Förster transfer energy dependence calculated from Eq. (4), referred to hereafter as model II. In both models,

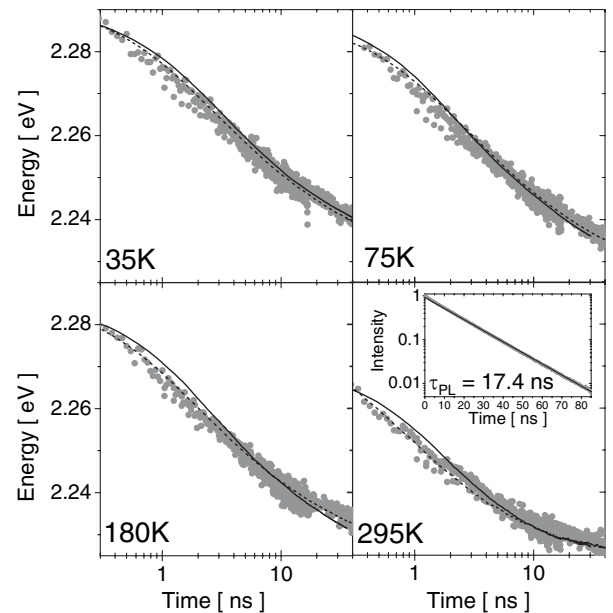


FIG. 2. Time evolution of mean PL energy (gray points) for thin films of AlQ3 at 295, 180, 75, and 35 K, showing fits to the mean PL energy using model I (solid black lines) and model II (dashed black lines), using the parameters listed in Table I. Inset: Integrated total PL intensity time decay data (gray dots) for the 295 K measurement with fit (black line).

we use the parameters τ , w_{DOS} , R_F , and E_0 , which is defined as the mean PL energy at time $t = 0$, the time when the excitation pulse arrives. At 295 K the PL lifetime (τ_{PL}) for AlQ3 is 17.4 ± 0.5 ns, obtained from a single exponential fit to the integrated PL intensity time decay, as shown in the inset of Fig. 2. Since τ is equal to τ_{PL} divided by the PL quantum efficiency [18], which is $32\% \pm 2\%$ [19] for AlQ3 thin films at 295 K, we find that $\tau = 54 \pm 4$ ns.

In the first set of numerical fits, model I is used. The fits were calculated using the analytic solution developed by Movaghar *et al.*, and then compared to MC simulations using Eqs. (1)–(4). We find that the MC and analytic results agree only if the MC simulation utilizes a cubic lattice of molecular sites [20]. The fitted time evolution of the mean PL energy is shown as a solid line in Fig. 2, and the corresponding values of R_F , w_{DOS} , and E_0 are listed in Table I.

A second set of fits, denoted by dashed lines in Fig. 2, were generated using model II, and the associated fitting parameters are again listed in Table I. In this model, a lattice of randomly spaced sites is used, with the restriction that no two sites can be closer than a minimum intermolecular distance D_{min} , which reflects the finite size of the molecules. We use $D_{\text{min}} = 0.70$ nm, based on an estimate of the minimum distance configuration of two AlQ3 molecules, using the ground state structure reported by Halls *et al.* [21]. The average site density is set to equal the AlQ3 density, which is 1.5×10^{21} cm $^{-3}$ based on a mass density of 1.16 g/cm 2 and a molecular weight of 459.4. Additionally, we replace the Boltzmann distribution in Eq. (2) with the Förster expression of Eq. (4). We measure $n = 1.70 \pm 0.02$ by ellipsometry of AlQ3 films, and use $\kappa^2 = 2/3$ to average over the random donor and acceptor orientations. Finally, since S_D and σ_A refer to molecular spectra, the observed bulk spectra can not be directly input into Eq. (4). Rather we must deconvolve $g(E)$ from the bulk absorption spectrum for AlQ3 to obtain σ_A . (In this

step, we assume that the energy spacing between the S_D and σ_A mean energies is the same for each molecule.) Obtaining S_D is more involved, since the bulk PL spectrum reflects both the molecular spectrum and the energy shifts due to exciton diffusion. However, our MC simulations output the energy distribution, $n_{\text{ex}}(E)$, of all the excitons emitted over the simulation time window (which matches the measurement window). We then obtain S_D by deconvolving $n_{\text{ex}}(E)$ from the bulk PL spectrum.

Having obtained the spectral shapes for σ_A and S_D , the final step in calculating the Förster transfer energy dependence is to properly locate the spectra in energy. In both models, the R_F value in Eq. (3) refers to transfer between two molecules in the center of the $g(E)$ distribution, which we designate as *median* molecules. For a median molecule, σ_A is centered under the bulk absorption spectrum, and S_D is centered at E_0 . Note that at $t = 0$, the exciton population is proportional to $g(E)$. Therefore, at this moment in time the mean PL energy of both the ensemble and the median molecule is equal to E_0 . Figure 3 shows the bulk and molecular spectra for the 295 K data fitted using model II, along with $g(E)$ and $n_{\text{ex}}(E)$. Note that this fitting process is iterative, whereby initial guesses for w_{DOS} and E_0 are made, the simulation carried out, S_D and σ_A deconvolved from the bulk spectra, and the fits and self-consistency evaluated.

From Fig. 2, we find that both models fit the experimentally observed data, but Table I shows that only model II is strictly self-consistent. For model II the R_F value used in each fit is consistent with the R_F^{calc} value (see Table I) obtained from Eq. (4), using the σ_A and S_D for median molecules. Such self-consistent fits were impossible to obtain using model I, with the parameters listed in Table I reflecting the fits that came the closest to achieving self-consistency. The fit values overestimate R_F as compared to R_F^{calc} by between 13% and 33%, corresponding to

TABLE I. Model parameters for fitting the dynamic redshift in the mean PL of thin films of AlQ $_3$ at different temperatures. Model I is after Movaghar *et al.* and model II is the model presented in this Letter, T is the temperature, R_F is the Förster radius, w_{DOS} is the FWHM of $g(E)$, E_0 is the mean PL energy at $t = 0$, and R_F^{calc} is the value for R_F calculated from Eq. (4).

Model	T (K)	R_F (nm)	w_{DOS} (eV)	E_0 (eV)	R_F^{calc} (nm)
I	295	1.26	0.081 ± 0.03	2.27	1.12 ± 0.05
I	180	1.20	0.077 ± 0.03	2.29	0.98 ± 0.05
I	75	1.26	0.068 ± 0.03	2.29	0.95 ± 0.05
I	35	1.22	0.062 ± 0.03	2.29	0.96 ± 0.05
II	295	1.12	0.092 ± 0.03	2.28	1.12 ± 0.05
II	180	0.95	0.092 ± 0.03	2.28	0.95 ± 0.05
II	75	0.90	0.092 ± 0.03	2.29	0.90 ± 0.05
II	35	0.90	0.092 ± 0.03	2.29	0.90 ± 0.05

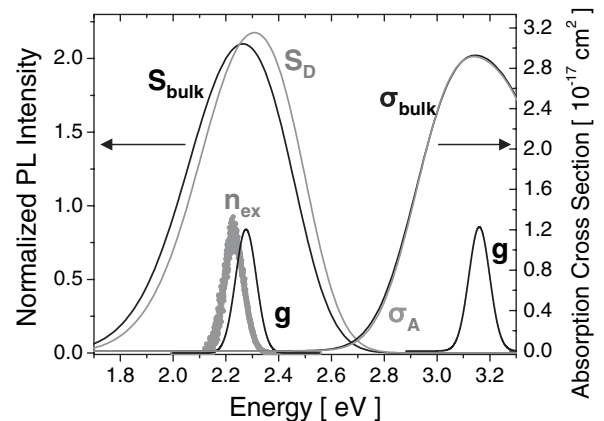


FIG. 3. Molecular AlQ $_3$ absorption (σ_A) and PL (S_D) spectra, calculated from 295 K data for the model II fit. Also shown are the bulk absorption (σ_{bulk}) and PL (S_{bulk}) spectra, as well as the DOS [$g(E)$] for absorption and emission, and the time integrated energy distribution of emitted excitons (n_{ex}).

errors in the Förster transfer rate of between 200% and 540% (through the sixth power dependence on R_F).

We further note that for model I, the w_{DOS} values decrease markedly with temperature, while for model II, they remain constant. Since the variations in the exciton energies are assumed to be due to molecular dipole interactions that are temperature independent, we expect w_{DOS} to also be temperature independent as we observe in model II. We conclude that in model I the use of the Boltzman distribution in the transfer rate equation [Eq. (2)] is the source of this inconsistent energy dependence.

In this Letter we considered exciton diffusion in fluorescent materials as dominated by Förster energy transfer. The primary additional diffusion mechanism is Dexter transfer, which arises as a result of correlated electron exchange between two molecules [22]. The Dexter transfer rate is usually much lower than the Förster transfer rate unless the transition dipole moment of the exciton is nearly zero, as in the case of triplet excitons in phosphorescent materials [18]. Since in AlQ3 PL measurements singlet excitons with strong transition dipole moments provide the observed PL signal, we conclude that the contribution to the exciton diffusion rate by Dexter transfer is negligible. Another alternative mechanism for the observed spectral shifts is an energy dependent exciton trapping process. However, the single exponential behavior observed in the PL intensity decay indicates that such a mechanism is not present; as such a trapping process would yield a time dependent quenching rate (see, e.g., [23]).

In summary, from the comparison of models I and II, we conclude that the use of the Boltzman distribution and cubic lattice approximations in modeling Förster transfer lead to errors in the values obtained for both R_F and w_{DOS} , requiring the modifications implemented in model II to achieve self-consistency. This Letter provides the first quantitative demonstration that directly calculating the Förster transfer rates from the overlap integral when modeling exciton diffusion with energy disorder, as done in recent polymer studies (see, e.g., [24,25]), is superior to the Boltzman distribution. To the author's knowledge, this is also the first report of a precise value for the excitonic w_{DOS} of a fluorescent amorphous molecular organic thin film. Finally, we note that while the Movaghar model has been

widely accepted and utilized for qualitative analyses, the model presented in this study provides the first quantitatively self-consistent model of exciton diffusion in organic solids with spatial and energetic disorder.

The authors thank Dr. Steve Kooi for his assistance. This work was supported in part by the NSF CAREER Grant, Graduate NDSEG Grant, and the MARCO Focused Research Center on Materials, Structures and Devices, with equipment provided by the U.S. Army through the MIT Institute for Soldier Nanotechnologies.

*Electronic address: bulovic@mit.edu

- [1] B. Movaghar, J. Phys. C **13**, 4915 (1980).
- [2] B. Movaghar *et al.*, Phys. Status Solidi B **97**, 533 (1980).
- [3] B. Movaghar *et al.*, Solid State Commun. **34**, 451 (1980).
- [4] B. Movaghar *et al.*, J. Phys. C **14**, 859 (1981).
- [5] B. Movaghar *et al.*, Phys. Rev. B **33**, 5545 (1986).
- [6] S. Heun *et al.*, J. Phys. Condens. Matter **5**, 247 (1993).
- [7] R. Kersting *et al.*, Phys. Rev. Lett. **70**, 3820 (1993).
- [8] B. Mollay *et al.*, Phys. Rev. B **50**, 10769 (1994).
- [9] M. Yan *et al.*, Phys. Rev. Lett. **73**, 744 (1994).
- [10] S. Meskers *et al.*, Chem. Phys. Lett. **339**, 223 (2001).
- [11] S. Meskers *et al.*, IEEE Trans. Dielectr. Electr. Insul. **8**, 321 (2001).
- [12] M. Ariu *et al.*, Phys. Rev. B **67**, 195333 (2003).
- [13] L. Herz *et al.*, Phys. Rev. B **70**, 165207 (2004).
- [14] H. Bassler *et al.*, Acc. Chem. Res. **32**, 173 (1999).
- [15] The idea of spatial disorder in exciton phenomena is not new. See, e.g., Bassler [16] for an early review of the subject, and Scheidler *et al.* [17] for a more recent study.
- [16] H. Bassler, Phys. Status Solidi B **107**, 9 (1981).
- [17] M. Scheidler *et al.*, Phys. Rev. B **54**, 5536 (1996).
- [18] M. Pope *et al.*, *Electronic Processes in Organic Crystals and Polymers* (Oxford University Press, New York, 1999).
- [19] D. Garbuzov *et al.*, Chem. Phys. Lett. **249**, 433 (1996).
- [20] The molecular density used in the analytic solution of model I must be scaled by a percolation factor, a_p [5]. In this work we find $a_p = 2.22$ yields good agreement with cubic lattice MC simulations.
- [21] M. Halls *et al.*, Chem. Mater. **13**, 2632 (2001).
- [22] D. L. Dexter *et al.*, J. Chem. Phys. **21**, 836 (1953).
- [23] R. Richert *et al.*, Philos. Mag. B **49**, L25 (1984).
- [24] D. Beljonne *et al.*, J. Phys. Chem. B **109**, 10594 (2005).
- [25] S. Westenhoff *et al.*, J. Chem. Phys. **122**, 094903 (2005).